Title

Computational study of p -xylene synthesis from ethylene and 2,5-dimethylfuran catalyzed by H-BEA

Authors

Li, YP
Head-Gordon, M
Bell, AT

Peer reviewed

Computational Study of *p*-Xylene Synthesis from Ethylene and 2,5-Dimethylfuran Catalyzed by H-BEA

Yi-Pei Li,[†] Martin Head-Gordon,[‡] and Alexis T. Bell*,[†]

[†]Department of Chemical and Biomolecular Engineering, University of California, Berkeley, California 94720-1462, United States
[‡]Department of Chemistry, University of California, Berkeley, California 94720-1462, United States

Ⓢ *Supporting Information*

ABSTRACT: Detailed mechanisms for the synthesis of *p*-xylene as well as the primary byproducts observed experimentally, 2,5-hexadione and 2,5-dimethyl-3-[(4-methyl-1,3-cyclohexadien-1-yl)methyl]furan, from ethylene and 2,5-dimethylfuran (DMF) mediated by H-BEA are obtained using an extended QM/MM model containing 208 tetrahedral atoms. The formation of *p*-xylene proceeds via Diels−Alder cycloaddition of ethylene and DMF, which is rate-limiting, followed by Brønsted acid-catalyzed dehydration. Secondary addition of DMF to the substrate following the Diels−Alder reaction leads to 2,5-dimethyl-3-[(4-methyl-1,3-cyclohexadien-1-yl)methyl]furan. The analysis of the free energies associated with the mechanisms suggests that the secondary addition can be eliminated by introducing *n*-heptane as an inert solvent to decrease the loading of DMF in the zeolite or by using a weak Brønsted acid site to facilitate the dehydration of the Diels−Alder product, for which the rate is determined by the deprotonation via the conjugate base of the active site. Water formed in the dehydration process can react directly with DMF to form 2,5-hexadione, thereby decreasing the yield of *p*-xylene. However, the free-energy barriers for the formation of 2,5-heaxdione compared to the Diels−Alder reaction indicate that DMF and 2,5-hexadione will be equilibrated. Therefore, the 2,5-hexadione yield can be minimized by operating at a high conversion of DMF.
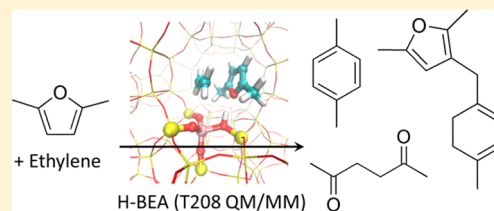
INTRODUCTION

p-Xylene is used primarily as a precursor of terephthalic acid, the monomer of polyethylene terephthalate (PET). Due to growth in the production of polyester fibers, the global demand for *p*-xylene has been steadily increasing and the improvement in technologies for *p*-xylene production has become an active research area.[1] Conventionally, *p*-xylene is produced along with *o*-xylene, *m*-xylene, and other aromatics by the catalytic reforming of the naphtha fraction of petroleum. However, due to the close boiling points of the xylene isomers, the separation of *p*-xylene is difficult and is done conventionally by crystallization or adsorption, steps that are energy intensive and expensive.[2] The cost of *p*-xylene separation could be alleviated if this product could be produced selectively. This goal is achievable by means of toluene disproportionation or toluene methylation.[2] An attractive alternative is the Diels−Alder cycloaddition of 2,5-dimethylfuran (DMF) and ethylene and subsequent dehydration of the resulting product. This process is catalyzed by Brønsted acid zeolites and produces *p*-xylene selectively.[3] Since both DMF and ethylene can be derived from lignocellulosic biomass, the production of *p*-xylene from DMF and ethylene is not dependent on petroleum and is, hence, a sustainable process.[3]

The production of *p*-xylene from DMF and ethylene has been estimated to be more economically feasible than the production of biobased *p*-xylene announced by GEVO Inc., which uses the fermentation of glucose followed by the catalytic conversion.[4] However, further optimization of the catalyst and better integration of the process are needed in order to bring the cost of *p*-xylene derived from DMF and ethylene closer to that for *p*-xylene derived from petroleum.[4] For example, while *p*-xylene is the sole xylene isomer obtained via the cycloaddition of ethylene to DMF, characterization of the reaction mixture by NMR and GC−MS has revealed two competing side reactions, as shown by Scheme 1.[5] During the dehydration of the oxa-

Scheme 1. Schematic Representations of the Reaction Network of the Production of *p*-Xylene from Dimethylfuran (DMF) and Ethylene Catalyzed by Brønsted Acid Zeolites
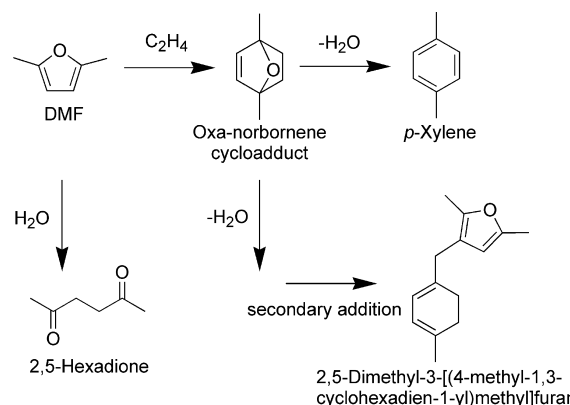
norbornene cycloadduct, the electrophilic intermediates can react with electron-rich compounds (e.g., DMF) to produce a variety of byproducts via secondary processes. 2,5-Dimethyl-3-[(4-methyl-1,3-cyclohexadien-1-yl)methyl]furan, the dimer molecule shown in Scheme 1, has been identified as the primary byproduct and is chosen as the representative of the collection of the byproducts from secondary addition in the present work.[5] Water produced in the dehydration steps can react with DMF to form 2,5-hexadione, further lowering the selectivity to *p*-xylene. However, it has been shown experimentally that the hydrolysis reaction is reversible so that if most of the DMF is consumed (i.e., high conversion of DMF is achieved), 2,5-hexadione reforms to DMF, reducing the yield of 2,5-hexadione.[6] It has also been shown that the formation of compounds from secondary addition can be suppressed by introducing *n*-heptane;[3] however, the reason why an inert aliphatic solvent helps to eliminate secondary addition is not clear.

To address this question, as well as to explore other possibilities for improving the selectivity to *p*-xylene, we have carried out a computational analysis of the energetics of *p*-xylene, 2,5-hexadione, and 2,5-dimethyl-3-[(4-methyl-1,3-cyclohexadien-1-yl)methyl]furan formation catalyzed by H-BEA, the zeolite system with which the highest yield of *p*-xylene was achieved.[6] This effort was carried out by means of quantum mechanics/molecular mechanics (QM/MM) calculations using a large cluster representation of the active site and the surrounding zeolite involving 208 tetrahedral atoms (T208) to capture the confinement and dispersion effects of the pores. Our work has identified reaction mechanisms that are consistent with the deductions drawn from experiments (Scheme 1). The associated free-energy surfaces show that the Diels−Alder cycloaddition of DMF and ethylene is the overall rate-limiting step with a free-energy barrier that is in very good agreement with that observed experimentally. Moreover, the apparent free-energy barrier of the Diels−Alder reaction is found to be much higher than both of the forward and backward free-energy barriers of the hydrolysis side reaction, which is consistent with the experimental observation that DMF and 2,5-hexadione are in equilibrium compared with the production of *p*-xylene. The analysis of the free-energy surface demonstrates that the selectivity to *p*-xylene could be improved by introducing *n*-heptane and suggests that further improvements in selectivity could be achieved by tuning the Brønsted acidity of the acid site.

■ THEORETICAL METHODS

Zeolite Model Geometries. The structure of BEA was described by a T208 cluster with the position of all Si and O atoms determined by the crystallographic structure of BEA.[7] The cluster was terminated with hydrogen atoms replacing the terminal oxygen atoms. H-BEA was produced by replacing a Si atom in the framework by an Al atom and introducing a proton to compensate the resulting charge imbalance. Although BEA has 9 unique T atom positions, two sites are suggested to be most favored energetically for Al atom substitution[8] (i.e., the T1 and T2 sites in the nomenclature of Newsam et al).[7] For this study, we considered the Al atom to be located in the T2 site.

QM/MM Computations. Implementation of the QM/MM model in this work followed the electrostatic embedding scheme described previously.[9] As shown in Figure 1, reactants and a T5 cluster encompassing the active center were described
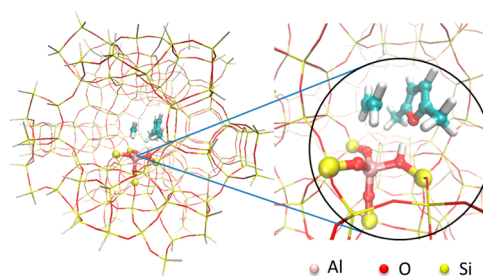

Figure 1. H-BEA QM/MM model (T208), where the T2 site is shown. Spherical atoms are QM atoms, others are MM atoms.

by QM, whereas the rest of the zeolite was described by MM using a standard force field of the CHARMM type.[10−12] All geometry optimizations were performed with relaxation of the atoms only in the QM region while maintaining all of the MM atoms frozen. The parameters for atoms of the zeolite cluster are listed in Table 1. These values have been recently

Table 1. Charge and Lennard-Jones Parameters for O and Si Used in the QM/MM Portion of This Work

Q_{Si}	Q_O	ε_{Si} (kcal/mol)	R_{Si} (Å)	ε_O (kcal/mol)	R_O (Å)
0.7	−0.35	0.047	2.2	0.018	1.77

reoptimized to yield improved accuracy for adsorption energies of organic molecules in zeolites and have been applied to study the isomerization of glucose to fructose catalyzed by Sn-BEA.[13,14] Standard CHARMM parameters were used for the atoms of the substrates.[15]

Geometry optimizations and single-point energy calculations were performed using density functional theory (DFT) at the ωB97X-D[16,17]/6-31G* and ωB97X-D/6-311++G(3df,3pd) levels of theory, respectively. All QM/MM calculations were carried out using a development version of the Q-Chem software package.[18] The initial geometries of reaction intermediates were manually guessed and then refined using gradient-based local optimizations. The transition structures connecting pairs of intermediates were then found by the freezing string method[19] followed by local optimization. Kinetically uncompetitive pathways were discarded and only the lowest energy pathway was retained. Free energies were determined using a quasi-RRHO approach.[13,20]

Solvation of Substrates. A previous study has shown that in addition to the gas-phase ethylene, liquid-phase DMF, and solid-phase zeolite, an aqueous phase is formed as the reaction proceeds, since the dehydration steps produce water.[3] To obtain a reasonable comparison with the experimentally measured reaction barrier, the free energy of the isolated catalyst and the solvated DMF, instead of DMF in gas phase, were chosen as the references for the free-energy surface

$$G = G(SC) - G(C) - G(\text{ethylene}) - G_{sol}(\text{DMF})$$

$$= G(SC) - G(C) - G(\text{ethylene})$$
$$- [G(\text{DMF}) + \Delta G_{\text{solvation}}(\text{DMF})] \quad (1)$$

where $G(X)$ is the free energy of species X in gas phase, SC stands for the substrate-catalyst complex, C stands for the catalyst, and $\Delta G_{\text{solvation}}(\text{DMF})$ is the free-energy difference of DMF in the organic (DMF or *n*-heptane) and gas phases. Similarly, the water and organic compounds produced in the reaction were assumed to be fully solvated in aqueous and
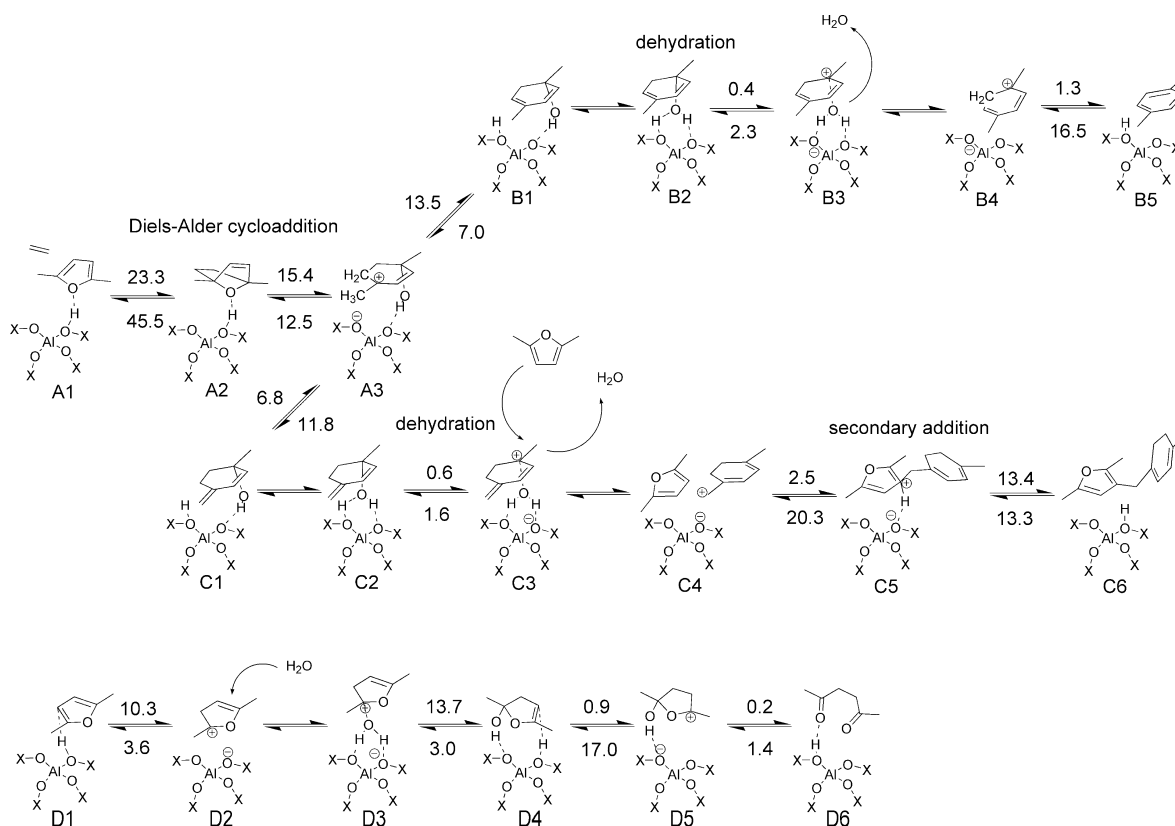
Figure 2. Mechanisms and energetics of the formation of *p*-xylene (B5), 2,5-hexadione (D6), and 2,5-dimethyl-3-[(4-methyl-1,3-cyclohexadien-1-yl)methyl]furan (C6) from DMF and ethylene mediated by the T2 site of H-BEA. Calculated ground state electronic energy barriers for each step (forward is the upper number, reverse is the lower number) are reported in kcal/mol. Barriers were not located for steps which do not involve covalent bond-making or breaking (and thus are not rate-determining).

organic (DMF or *n*-heptane) phases, respectively, after desorbing from the solid-phase zeolite. To simplify the problem, the aqueous and organic phases are assumed to be mutually immiscible, and the solutions are assumed to be ideal. $\Delta G_{solvation}$ was calculated using classical molecular dynamics (MD) simulations with force field from the SwissParam server[15] and the Bennett acceptance ratio (BAR) method.[21] All the MD simulations were performed using GROMACS.[22]

■ RESULTS AND DISCUSSION

Reaction Mechanism. The lowest-energy mechanisms for the formation of *p*-xylene, 2,5-hexadione, and 2,5-dimethyl-3-[(4-methyl-1,3-cyclohexadien-1-yl)methyl]furan from DMF and ethylene mediated by the H-BEA are shown in Figure 2. The transition states which do not involve cleavage and/or formation of covalent bonds (e.g., states B1 to B2) are not likely to be rate-limiting and, therefore, were not determined. The formation of *p*-xylene starts with a Diels−Alder cycloaddition, followed by a proton transfer from the active site to the oxa-norbornene, the species shown by state A2, resulting in ring-opening of oxa-norbornene cycloadduct. In the ring-opening step, which begins with state A3, the positively charged substrate is deprotonated to form a species with conjugated double bonds. If the proton on the ring is transferred to the active site, conjugated double bonds are formed on the ring, state B1. Then, following Brønsted acid-catalyzed dehydration from states B1 to B5, *p*-xylene is formed.

On the other hand, if the methyl group in state A3 is deprotonated, it forms a methylene group conjugated with the double bond on the ring, state C1. Following Brønsted acid-catalyzed dehydration via states C1 to C3, the positive charge on the species C3 can migrate to the methyl group, the position with least steric hindrance for addition reactions. Then, an electron-rich molecule, such as DMF, can attack this electrophile easily to form states C4 to C5, a process with a barrier of only 2.5 kcal/mol. The deprotonation of species C5 leads to 2,5-dimethyl-3-[(4-methyl-1,3-cyclohexadien-1-yl)methyl]-furan, the primary byproduct observed experimentally. For the reaction network shown in Figure 1, the initiation step (Diels−Alder cycloaddition) is the one with the highest barrier, 23.3 kcal/mol.

The hydrolysis of DMF starts with the protonation at the *β*-position of DMF, followed by nucleophilic attack of the water molecule at the *α*-position as illustrated by states D1 to D3 in Figure 2. This finding is consistent with the mechanism recently proposed by Nikbin et al. for the hydrolysis of DMF catalyzed by Brønsted acids in aqueous solution.[23] The proton transfer after the nucleophilic attack from the water to the active site regenerates the Brønsted acid site, allowing the second protonation at the *β*-position to occur, as shown by states D3 to D5. The last step is the proton transfer from hydroxyl group at the *α*-position to the active site, results in a concerted ring-opening of species D5 to form 2,5-hexadione.

Free-Energy Surface. Figure 3 shows the free-energy surface for the formation of *p*-xylene and the dimer, 2,5-dimethyl-3-[(4-methyl-1,3-cyclohexadien-1-yl)methyl]furan, at the experimental conditions (573 K, 57 bar)[3] without additional solvent. Under these conditions, the reaction system is composed of the gas-phase ethylene, the liquid-phase DMF,
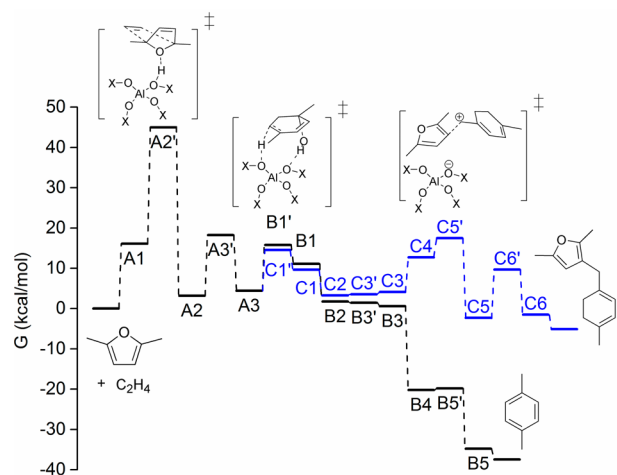
Figure 3. Free-energy surface (573 K, 57 bar, 1 M in DMF) of the formation of *p*-xylene and 2,5-dimethyl-3-[(4-methyl-1,3-cyclohexa-dien-1-yl)methyl]furan from DMF and ethylene mediated by the T2 site of H-BEA. The states noted with a prime symbol are transition states. For instance, state A2′ is the transition state connecting intermediates A1 and A2.

and solid-phase zeolite. All organic products are assumed to be dissolved in DMF, as is the byproduct water formed via dehydration. The reference-state concentration chosen for all solutes is 1 M. As shown in Figure 3, since the free energy of the transition state A2′ is the highest one along the reaction pathway, we conclude that the rate-limiting step is the Diels−Alder cycloaddition. This finding is consistent with the conclusion drawn previously based on gas-phase DFT calculations for the conversion of DMF and ethylene to *p*-xylene catalyzed by a proton.[24] The apparent free-energy barrier for this step is 45.0 kcal/mol, which is in very good agreement with the experimental value of 44.3 kcal/mol (see Text S1 of the Supporting Information for how this number is derived).

It is also shown in Figure 3 that the free-energy difference between states C5′ and B1′, $\Delta G(\text{C5}'\text{-B1}')$, determines the selectivity to *p*-xylene since the free energies of the transition states C5′ and B1′ are the highest points along the two divergent pathways starting from A3. To maximize the selectivity to *p*-xylene, a large value of $\Delta G(\text{C5}'\text{-B1}')$ is desired. This can be achieved by either introducing a good solvent for DMF or using a weak Brønsted acid site. Introducing a good solvent for DMF decreases the loading of DMF in the zeolite system, resulting in a lower probability for forming the complex C5′ (i.e., a higher free energy for transition state C5′). As shown in Table 2, at the same conditions (573 K, 57 bar, 1 M for all solutes), $\Delta G(\text{C5}'\text{-B1}')$ increases from 1.7 to 2.2 kcal/mol if *n*-heptane is used as the solvent, resulting in a 1.5-fold increase in the ratio of the formation rate of *p*-xylene to the

dimer comparing with the DMF case. On the other hand, as shown in Table 2, a 2-fold increase in this ratio can be achieved by substituting Al in the active site with Ga, which is known as a weaker Brønsted acid site.[25] This is because the transition state B1′ corresponds to a deprotonation reaction mediated by the conjugate base of the acid site. If a weaker Brønsted acid site is used, the conjugate base is stronger so that the deprotonation process leading to *p*-xylene becomes more strongly preferred.

We note that the free-energy differences discussed above are not very large. For example, the difference in $\Delta G(\text{C5}'\text{-B1}')$ between using DMF and *n*-heptane as solvents is 0.5 kcal/mol, a value close to the limit of the chemical accuracy attainable from either computations or experiments. However, since the number represents the difference in free energy between two free-energy changes calculated by identical methodology, higher accuracy can be expected because systematic errors in the theoretical predictions should cancel. Therefore, the trends in the free energies discussed above should be valid. This conclusion is supported by the observation that the predicted trends with changes in solvent composition are consistent with reported experimental observations.

The selectivity to *p*-xylene can further be increased if Al is substituted by B because the Brønsted acidity of the B site is weaker than the Ga site.[25] However, as tabulated in Table 2, the overall reaction rate is greatly decreased if B-BEA is used because the Brønsted acidity of the site determines the adsorption free energy of DMF (i.e., the free energy of state A1), affecting the apparent free-energy barrier of the Diels−Alder cycloaddition. Therefore, we note that while a Brønsted acid site does not facilitate Diels−Alder cycloaddition, since the intrinsic free-energy barrier for Diels−Alder cycloaddition, $\Delta G(\text{A2}'\text{-A1})$, over a siliceous BEA is close to that for Brønsted acid sites, the overall reaction rate is greatly decreased if B-BEA or Si-BEA is used because the strength of reactant adsorption is weaker than in Al-BEA. Therefore, considering both the reactivity and the selectivity to *p*-xylene, Ga-BEA is recommended based on our calculations.

The free-energy surface of the hydrolysis side reaction was also calculated (Figure S1 of the Supporting Information), and the forward and backward apparent free-energy barriers were found to be 28.2 and 20.5 kcal/mol, respectively, which are both much smaller than the apparent free-energy barrier of the Diels−Alder cycloaddition (45.0 kcal/mol), suggesting that DMF and 2,5-hexadione, the byproduct from the hydrolysis of DMF, are in rapid equilibrium compared with the formation of *p*-xylene. This finding is consistent with the experimental observation that the yield of 2,5-hexadione can be reduced by working at a high conversion of DMF.[6]

One may notice that there are two negative free-energy barriers in Figure 3, the transition from B2 to B3′ and from C3 to C3′. For these two steps, as shown by Figure 2, the electronic energy difference between the transition state and

Table 2. Effects of Brønsted Acidity and Solvents on the Reaction Rate of Diels-Alder Cycloaddition and the Selectivity to *p*-Xylene

	solvent	G(A1) (kcal/mol)	$\Delta G(\text{A2}'\text{-A1})$ (kcal/mol)	r(Diels−Alder) (1/s)	$\Delta G(\text{C5}'\text{-B1}')$ (kcal/mol)	r(*p*-xylene) /r(dimer)
Al	DMF	16.1	28.9	8.3×10^{-5}	1.7	4.4
Al	*n*-heptane	16.6	28.9	5.3×10^{-5}	2.2	6.8
Ga	DMF	16.2	28.7	8.9×10^{-5}	2.6	9.7
B	DMF	21.0	31.1	1.6×10^{-7}	4.5	53.8
Si	DMF	21.4	30.7	1.6×10^{-7}		

the intermediate is small so that the relative height of the transition state and intermediate can be inverted once the entropy and the zero-point vibrational and thermal corrections are taken into account in the free-energy diagram. Since these two steps are kinetically irrelevant, no action was taken to correct the artifact.

CONCLUSIONS

Detailed mechanisms for the formation of *p*-xylene, 2,5-hexadione, and 2,5-dimethyl-3-[(4-methyl-1,3-cyclohexadien-1-yl)methyl]furan, the primary byproduct observed experimentally, from DMF and ethylene mediated by the H-BEA and the associated free-energy surfaces have been obtained using QM/MM simulations. The formation of *p*-xylene consists of a Diels−Alder cycloaddition followed by Brønsted acid-catalyzed dehydration (see Figure 2). The Diels−Alder cycloaddition, which requires an apparent free-energy barrier of 45.0 kcal/mol, is rate-limiting for the overall reaction. The subsequent dehydration process produces water, which can hydrolyze DMF to form 2,5-hexadione. However, because the apparent free-energy barriers for forward and backward reaction involved in the hydrolysis side reaction (28.2 and 20.5 kcal/mol) are both much smaller than that for Diels−Alder cycloaddition, DMF and 2,5-hexadione rapidly reach equilibrium. Therefore, the yield of 2,5-hexadione can be minimized by operating at a high conversion of DMF. The primary byproduct, 2,5-dimethyl-3-[(4-methyl-1,3-cyclohexadien-1-yl)methyl]furan, is formed if after the Diels−Alder cycloaddition, the substrate condenses with another molecule of DMF (see Figure 2). This secondary addition process can be eliminated by introducing *n*-heptane as an inert solvent to decrease the loading of DMF in the zeolite or by using a weak Brønsted acid site to facilitate the dehydration process, for which the reaction rate is determined by deprotonation triggered by the conjugated base of the active site. However, use of a weak Brønsted acid is not desirable for the overall reaction rate because the adsorption of DMF on a weak Brønsted acid site is less preferred, resulting in a higher apparent free-energy barrier of the Diels−Alder cycloaddition. Therefore, considering both the reactivity and the selectivity to *p*-xylene, BEA containing Ga is preferred over BEA containing Al or B, the strongest and weakest Brønsted acid sites considered (see Table 2).

ASSOCIATED CONTENT

Ⓢ Supporting Information

Additional information as noted in the text, including apparent free-energy barrier calculations and the free-energy diagram of the hydrolysis of DMF. This material is available free of charge via the Internet at http://pubs.acs.org.

AUTHOR INFORMATION

Corresponding Author

*E-mail: alexbell@berkeley.edu.

Notes

The authors declare no competing financial interest.

ACKNOWLEDGMENTS

REFERENCES

(1) Wantanachaisaeng, P.; O'Neil, K. *Capturing Opportunities for Para-Xylene Production*; Technical Report; UOP: A Honeywell Company: Des Plaines, IL, 2010.

(2) Ashraf, M. T.; Chebbi, R.; Darwish, N. A. Process of P-Xylene Production by Highly Selective Methylation of Toluene. *Ind. Eng. Chem. Res.* **2013**, *52*, 13730−13737.

(3) Williams, C. L.; Chang, C.-C.; Do, P.; Nikbin, N.; Caratzoulas, S.; Vlachos, D. G.; Lobo, R. F.; Fan, W.; Dauenhauer, P. J. Cycloaddition of Biomass-Derived Furans for Catalytic Production of Renewable P-Xylene. *ACS Catal.* **2012**, *2*, 935−939.

(4) Lin, Z.; Nikolakis, V.; Ierapetritou, M. Alternative Approaches for P-Xylene Production from Starch: Techno-Economic Analysis. *Ind. Eng. Chem. Res.* **2014**, *53*, 10688−10699.

(5) Do, P. T. M.; McAtee, J. R.; Watson, D. A.; Lobo, R. F. Elucidation of Diels−Alder Reaction Network of 2,5-Dimethylfuran and Ethylene on HY Zeolite Catalyst. *ACS Catal.* **2013**, *3*, 41−46.

(6) Chang, C.-C.; Green, S. K.; Williams, C. L.; Dauenhauer, P. J.; Fan, W. Ultra-Selective Cycloaddition of Dimethylfuran for Renewable P-Xylene with H-BEA. *Green Chem.* **2014**, *16*, 585−588.

(7) Newsam, J. M.; Treacy, M. M. J.; Koetsier, W. T.; Gruyter, C. B. D. Structural Characterization of Zeolite Beta. *Proc. R. Soc. London, Ser. A* **1988**, *420*, 375−405.

(8) Xiu-Liang, S.; Chong-Pin, H.; Jie, Z.; Biao-Hua, C. Location of Al and Acid Strength of Bronsted Acid in Beta Zeolite. *Acta Phys.-Chim. Sin.* **2009**, *25*, 1136−1142.

(9) Zimmerman, P. M.; Head-Gordon, M.; Bell, A. T. Selection and Validation of Charge and Lennard-Jones Parameters for QM/MM Simulations of Hydrocarbon Interactions with Zeolites. *J. Chem. Theory Comput.* **2011**, *7*, 1695−1703.

(10) Foloppe, N.; MacKerell, A. D., Jr. All-Atom Empirical Force Field for Nucleic Acids: I. Parameter Optimization Based on Small Molecule and Condensed Phase Macromolecular Target Data. *J. Comput. Chem.* **2000**, *21*, 86−104.

(11) Yin, D.; MacKerell, A. D. Combined Ab Initio/Empirical Approach for Optimization of Lennard−Jones Parameters. *J. Comput. Chem.* **1998**, *19*, 334−348.

(12) Vanommeslaeghe, K.; Hatcher, E.; Acharya, C.; Kundu, S.; Zhong, S.; Shim, J.; Darian, E.; Guvench, O.; Lopes, P.; Vorobyov, I.; et al. CHARMM General Force Field: A Force Field for Drug-like Molecules Compatible with the CHARMM All-Atom Additive Biological Force Fields. *J. Comput. Chem.* **2010**, *31*, 671−690.

(13) Li, Y.-P.; Gomes, J.; Sharada, S. M.; Bell, A. T.; Head-Gordon, M. *J. Phys. Chem. C*, to be submitted for publication.

(14) Li, Y.-P.; Head-Gordon, M.; Bell, A. T. Analysis of the Reaction Mechanism and Catalytic Activity of Metal-Substituted Beta Zeolite for the Isomerization of Glucose to Fructose. *ACS Catal.* **2014**, *4*, 1537−1545.

(15) Zoete, V.; Cuendet, M. A.; Grosdidier, A.; Michielin, O. SwissParam: A Fast Force Field Generation Tool for Small Organic Molecules. *J. Comput. Chem.* **2011**, *32*, 2359−2368.

(16) Chai, J.-D.; Head-Gordon, M. Long-Range Corrected Hybrid Density Functionals with Damped Atom−atom Dispersion Corrections. *Phys. Chem. Chem. Phys.* **2008**, *10*, 6615−6620.

(17) Chai, J.-D.; Head-Gordon, M. Systematic Optimization of Long-Range Corrected Hybrid Density Functionals. *J. Chem. Phys.* **2008**, *128*, 084106−084115.

(18) Shao, Y.; Molnar, L. F.; Jung, Y.; Kussmann, J.; Ochsenfeld, C.; Brown, S. T.; Gilbert, A. T. B.; Slipchenko, L. V.; Levchenko, S. V.; O'Neill, D. P.; et al. Advances in Methods and Algorithms in a Modern Quantum Chemistry Program Package. *Phys. Chem. Chem. Phys.* **2006**, *8*, 3172−3191.

(19) Behn, A.; Zimmerman, P. M.; Bell, A. T.; Head-Gordon, M. Efficient Exploration of Reaction Paths via a Freezing String Method. *J. Chem. Phys.* **2011**, *135*, 224108.

(20) Grimme, S. Supramolecular Binding Thermodynamics by Dispersion-Corrected Density Functional Theory. *Chem.—Eur. J.* **2012**, *18*, 9955−9964.

(21) Bennett, C. H. Efficient Estimation of Free Energy Differences from Monte Carlo Data. *J. Comput. Phys.* **1976**, *22*, 245−268.

(22) Pronk, S.; Páll, S.; Schulz, R.; Larsson, P.; Bjelkmar, P.; Apostolov, R.; Shirts, M. R.; Smith, J. C.; Kasson, P. M.; Spoel, D. van der; et al. GROMACS 4.5: A High-Throughput and Highly Parallel Open Source Molecular Simulation Toolkit. *Bioinformatics* **2013**, *29*, 845−854.

(23) Nikbin, N.; Caratzoulas, S.; Vlachos, D. G. On the Brønsted Acid-Catalyzed Homogeneous Hydrolysis of Furans. *ChemSusChem* **2013**, *6*, 2066−2068.

(24) Nikbin, N.; Do, P. T.; Caratzoulas, S.; Lobo, R. F.; Dauenhauer, P. J.; Vlachos, D. G. A DFT Study of the Acid-Catalyzed Conversion of 2,5-Dimethylfuran and Ethylene to P-Xylene. *J. Catal.* **2013**, *297*, 35−43.

(25) Jungsuttiwong, S.; Lomratsiri, J.; Limtrakul, J. Characterization of Acidity in [B], [Al], and [Ga] Isomorphously Substituted ZSM-5: Embedded DFT/UFF Approach. *Int. J. Quantum Chem.* **2011**, *111*, 2275−2282.